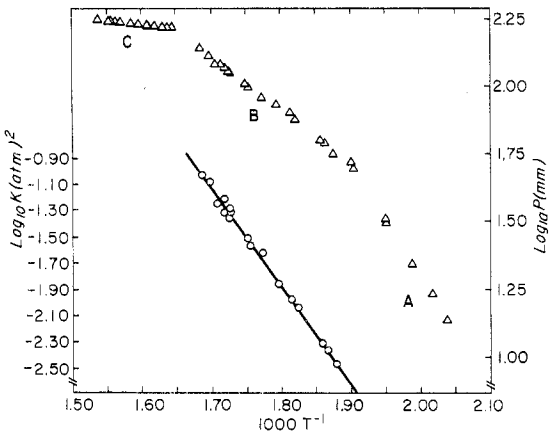

Figure 5. Total pressures represented by the open triangles (using the ordinate scale on the right) developed at various temperatures above a mixture of 2.26×10^{-5} mol of $AlCl_3$ and 5.5×10^{-5} mol of NH_4Cl in a diaphragm gauge of volume 25.3 cm^3. See text for discussion of regions A, B, and C. The open circles represent the same data in region B plotted (using the ordinate scale on the left) as the equilibrium constant for the reaction $NH_4^+(l) + Cl^-(l) \rightleftarrows NH_3(g) + HCl(g)$.

$$X_{NH_4^+} = X_{AlCl_4^-} + X_{Cl^-} = 1 - X_3$$

These equations are sufficient to define the system. The mole fraction of the ammine derived for the liquid phase varied from 0.6 at 531°K to 0.2 at 570°K. An equilibrium constant for the vaporization of "NH_4Cl" from the liquid phase can now be considered, i.e., reaction 4

$$\frac{K_4}{(RT/V)^2} = \frac{n_{HCl(g)} n_{NH_3(g)}}{X_{NH_4^+} X_{Cl^-}}$$

log K_4 values so derived are plotted *vs.* $1/T$ in Figure 5. The least-squares line leads to a $\Delta H°$ value of 34.3 ± 1.0 kcal mol^{-1} and $\Delta S°$ of 53.3 ± 1.3 cal mol^{-1} deg^{-1}.

No direct study of the vaporization equilibrium for pure liquid NH_4Cl has been found for comparison. The melting point under pressure is reported to be 793°K.[4] If the present results are combined with sublimation data, without correction for temperature or pressure differences, values for fusion of 5.3 ± 1.0 kcal mol^{-1} and 8.6 ± 1.3 cal deg^{-1} mol^{-1} are derived. The latter predict a melting point of 609°K; however, the uncertainties are large and values can be varied within the range indicated so as to yield the reported melting point.

One expects that use of the mole fraction in the treatment described will tend to underestimate the entropy of the mixture. In the dilute solution range (calculted Cl^- mole fractions range between 0.05 and 0.4) chloride ions were assumed to mix ideally with $AlCl_4^-$ ions, which are substantially larger. Because of the different ionic volumes the effective partial molar entropy of Cl^- in such a solution should be larger than it is in pure liquid NH_4Cl. A simple free volume ratio of 4 would provide a correction of 2.7 cal mol^{-1} deg^{-1} which overcorrects the entropy in the direction of predicting the correct melting point. An attempt to treat the data using volume fractions led to an intractable equation (seventh power) and results were apparently not sufficiently precise to give a meaningful solution. The simple solution model seems, however, to give a surprisingly good basis for correlating the vapor pressures generated by this mixture.

Acknowledgment. This work was carried out with financial assistance from the national Science Foundation, Grant 37033X, which is acknowledged with thanks.

Registry No. NH_4AlCl_4, 7784-14-7; $AlCl_3$, 7446-70-0; NH_4Cl, 12125-02-9; NH_3AlCl_3, 15550-69-3.

References and Notes

(1) E. Baud, *Ann. Chim. Phys.* **1**, No. 8, 8 (1904).
(2) K. N. Semeneko, W. N. Surov, and H. S. Kedrova, *Russ. J. Inorg. Chem.*, **14**, 481 (1969).
(3) Y. Yamaguti and S. Sisido, *J. Chem. Soc. Jpn.*, **62**, 304 (1941).
(4) D. R. Stull and H. Prophet, *Natl. Stand. Ref. Data Ser., Natl. Bur. Stand.*, **No. 37** (1971).
(5) I. S. Morozov and D. Ya. Toptygin, *Zh. Neorg. Khim.*, **3**, 1937 (1958).
(6) L. Y. Sob, *Russ. J. Inorg. Chem.*, **5**, 1353 (1960).
(7) A. V. Suvarov and V. L. Shybaev, *Probl. Sovrem. Khim. Koord. Soedin.*, **No. 2**, 76 (1968).
(8) H. L. Friedman and H. Taube, *J. Am. Chem. Soc.*, **72**, 2236 (1950).
(9) R. R. Richards and N. W. Gregory, *J. Phys. Chem.*, **68**, 3089 (1964).
(10) R. R. Richards, Doctoral Dissertation, University of Washington, Seattle, Wash. 98195 (1964).
(11) W. C. Laughlin and N. W. Gregory, *J. Chem. Eng. Data*, **20**, 137 (1975).
(12) W. C. Laughlin, Doctoral Dissertation, University of Washington, Seattle, Wash. 98195 (1974).

Contribution from the Department of Chemistry, University of Wyoming, Laramie, Wyoming 82081

Electronic Structure and Optical Properties of Manganese(V) Oxytrichloride, $MnOCl_3$

JERRY P. JASINSKI* and SMITH L. HOLT

Received September 25, 1974 AIC40675P

The electronic absorption spectrum of manganese(V) oxytrichloride, $MnOCl_3$, in the gas phase has been measured in the energy region from 12,000 to 52,000 cm^{-1}. The ground-state molecular orbital energy levels and transition-state energies have been calculated by the SCF–Xα scattered-wave method. Good agreement between the observed bands in the optical spectrum and the excitations from the transition-state Xα calculation is observed.

Introduction

A number of studies of the electronic structures of tetrahedral oxy anions containing Mn(V)[1-11] have been made. The most successful of these have centered around the polarized optical spectrum of MnO_4^{3-} doped into various crystalline tetrahedral hosts. Polarized optical spectra have helped to provide information which allows for a theoretical interpretation of the electronic structure of these systems.

Little is known, however, about the electronic structure of the symmetry-reduced oxyhalide analogs of the hypomanganate ion. In an effort to provide an explanation of the electronic structure of these analogs, we wish to report for the first time the optical absorption spectrum of manganese oxide trichloride, $MnOCl_3$, in the gas phase.

Calculational Method

In the past few years the SCF–Xα scattered-wave method has been used to describe the electronic structure of many systems, generally with good results. We have applied this method recently to CrO_2X_2 (X = F, Cl),[12] MnO_3X (X = F, Cl),[13] and MnO_2Cl_2[14] in an effort to explain the electronic

* Associated Western Universities Predoctoral Fellow at the Los Alamos Scientific Laboratory. Address correspondence to this author at the Department of Chemistry, University of Virginia, Charlottesville, Va. 22901.

Table I. Basis Functions for MnO_3F and MnO_3Cl in the SCF-Xα-SW Method: Normalized Symmetry Orbitals for Approximate Irreducible Representations

Centers	A_1	A_2	E
Outer	s	$f_{y(3x^2-y^2)}$	p_x
	p_z		d_{xz}
	$d_{(3z^2-r^2)}$		$d_{(x^2-y^2)}$
	$f_{z(5z^2-r^2)}$		$f_{x(5z^2-r^2)}$
	$f_{x(x^2-3y^2)}$		$f_{z(x^2-y^2)}$
Manganese	s	$f_{y(3x^2-y^2)}$	p_x
	p_z		d_{xz}
	$d_{(3z^2-r^2)}$		$d_{(x^2-y^2)}$
	$f_{z(5z^2-r^2)}$		$f_{x(5z^2-r^2)}$
	$f_{x(x^2-3y^2)}$		$f_{z(x^2-y^2)}$
Oxygen	s		p_x
	p_z		
Chlorine	$(1/\sqrt{3})$s(Cl1) + $(1/\sqrt{3})$s(Cl2) + $(1/\sqrt{3})$s(Cl3)	$(1/\sqrt{3})p_y$(Cl1) − $(1/2)p_x$(Cl2) − $(1/2\sqrt{3})p_y$(Cl2) + $(1/2)p_x$-(Cl3) − $(1/2\sqrt{3})p_y$(Cl3)	$(2/\sqrt{6})$s(Cl1) − $(1/\sqrt{6})$s(Cl2) − $(1/\sqrt{6})$s(Cl3)
	$(1/\sqrt{3})p_z$(Cl1) + $(1/\sqrt{3})p_z$(Cl2) + $(1/\sqrt{3})p_z$(Cl3)		$(2/\sqrt{6})p_z$(Cl1) − $(1/\sqrt{6})p_z$(Cl2) − $(1/\sqrt{6})p_z$(Cl3)
	$(1/\sqrt{3})p_x$(Cl1) − $(1/2\sqrt{3})p_x$(Cl2) + $(1/2)p_y$(Cl2) − $(1/2\sqrt{3})p_x$(Cl3) − $(1/2)p_y$(Cl2)		$(2/\sqrt{6})p_x$(Cl1) + $(1/2\sqrt{6})p_x$(Cl2) − $(1/2\sqrt{2})p_y$(Cl2) + $(1/2\sqrt{6})p_x$-(Cl3) + $(1/2\sqrt{2})p_y$(Cl3)
			$(3/2\sqrt{2})p_x$(Cl2) + $(1/2\sqrt{2})p_y$(Cl2) + $(\sqrt{3}/2\sqrt{2})p_x$(Cl3) − $(1/2\sqrt{2})p_y$(Cl3)

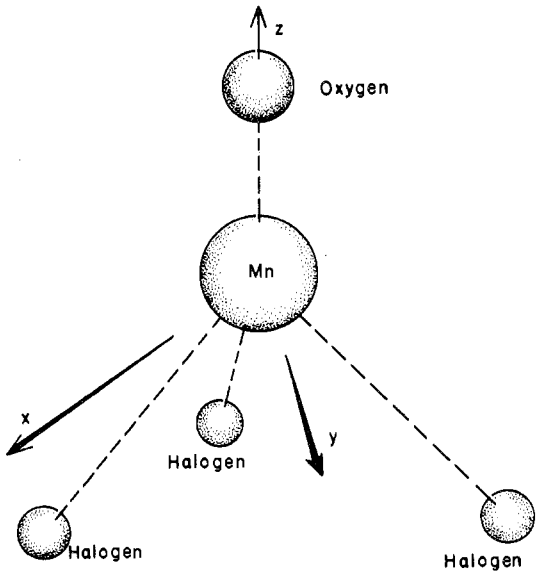

Figure 1. Coordinate system for a molecule with C_{3v} symmetry. [Mn-O = 1.56 Å, Mn-Cl = 2.12 Å, and O-Mn-Cl = 100° 12′ chosen by analogy to $VOCl_3$.[19,20] Coordinates (au): Mn (0, 0, 0), O (0, 0, a), Cl1 (b, 0, $-e$), Cl2 ($-d$, c, $-e$), Cl3 ($-d$, $-c$, $-e$) where a = 2.9478458, b = 2.8056326, c = 3.2957745, d = 1.9028163, and e = 1.2512283.]

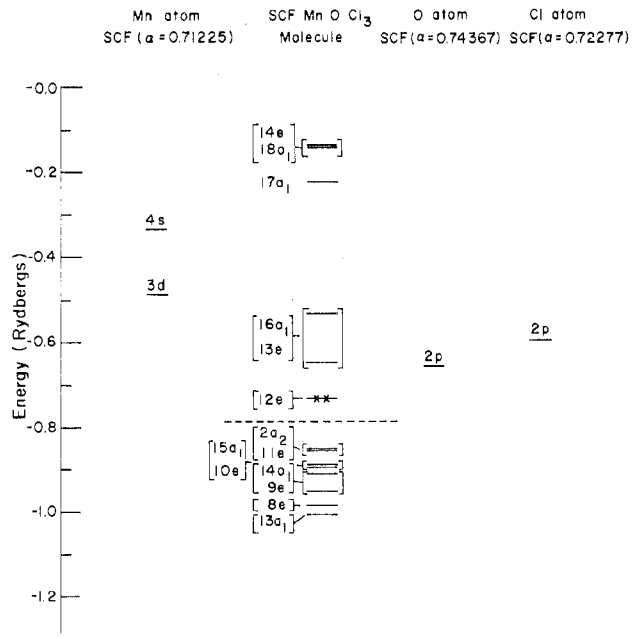

Figure 2. SCF-Xα-SW electronic "noncore" ground-state energy levels (in rydbergs) for a $MnOCl_3$ molecule in the gas phase. The energies are labeled according to the various irreducible representations of a C_{3v} symmetry group and are grouped according to a tetrahedral format. The highest fully occupied set of levels in the ground state is $2a_2^2$, $11e^4$. The $12e^2$ orbital is half-occupied while all other orbitals above the dashed line are unoccupied. Also shown are the corresponding SCF-Xα energy levels of the free atoms. [Sphere radii (au): outer sphere, 6.95390; Mn, 1.68935; Cl, 2.74755; O, 1.25850. α values: outer sphere, 0.72485; inner sphere, 0.72485.]

structure of molecules symmetry reduced from the parent CrO_4^{2-}, MnO_4^-, and MnO_4^{2-} ions, respectively. Our present application of the SCF-Xα method is an attempt to relate the electronic structure of $MnOCl_3$ to the parent MnO_4^{3-} ion. Our application of the method has been discussed in our earlier work,[12-14] while a more exhaustive treatment may be obtained in ref 15-18.

The structure of manganese oxide trichloride can be regarded as a low-symmetry perturbation of the MnO_4^{3-} cluster. Since little is known about the structure of $MnOCl_3$, its symmetry was assumed to be C_{3v}; see Figure 1. The sphere radii, exchange parameters (α values), and coordinate system were chosen in a manner similar to that for CrO_2Cl_2[12] and MnO_4^- [15] (cf. Figures 1 and 2). The oxygen radius was identical with that used by Johnson[15] (r_0 = 2.3552501 au). The Mn-O distance then uniquely determines the manganese radius (using touching spheres) and the Mn-Cl distance determines the chlorine radius. The sum of the Mn-Cl internuclear distance and the chlorine radius then determines the extramolecular (outer) sphere radius. The α values within the atomic spheres were taken from those for the free atoms tabulated by Schwarz.[21] For the inner-sphere region α was taken as a weighted sum (1 part of Mn, 1 part of O, and 3 parts of Cl) of Schwarz's values listed for these atoms. For the outer-sphere region α was taken as 1 part of oxygen and 3 parts of chlorine. The basis set (LCAO form) for the symmetry-correct orbitals from which the appropriate molecular orbitals are formed is given in Table I. These have been formed with reference to a set of local coordinate systems each of which is parallel to the coordinate system in Figure 1.

The ground-state molecular orbital eigenvalues resulting

Table II. SCF–Xα–SW Electronic Energy Levels (in Rydbergs) for a $MnOCl_3$ Molecule in the Gas Phase[a]

Symmetry	Occupancy	MO eigenvalues
14e	0	−0.1363
$18a_1$	0	−0.1382
$17a_1$	0	−0.2200
$16a_1$	0	−0.5325
13e	0	−0.6472
12e	2	−0.7323
$2a_2$	2	−0.8509
11e	4	−0.8530
$15a_1$	2	−0.8873
10e	4	−0.8923
$14a_1$	2	−0.9073
9e	4	−0.9515
8e	4	−0.9829
$13a_1$	2	−1.0572
7e (Cl 3s)	4	−1.7389 (−1.4675)
$12a_1$ (Cl 3s)	2	−1.7483 (−1.4675)
$11a_1$ (O 2s)	2	−2.0149 (−1.7305)
6e (Mn $3p_x$, $3p_y$)	4	−4.3857 (−3.9521)
$10a_1$ (Mn $3p_z$)	2	−4.3916 (−3.9521)
$9a_1$ (Mn 3s)	2	−6.5611 (−6.1260)
5e (Cl $2p_x$, $2p_y$)	4	−14.3684 (−14.1610)
4e (Cl $2p_x$, $2p_y$)	4	−14.3684 (−14.1610)
$1a_2$ (Cl $2p_x$, $2p_y$)	2	−14.3684 (−14.1610)
$8a_1$ (Cl $2p_x$, $2p_y$)	2	−14.3684 (−14.1610)
$7a_1$ (Cl $2p_z$)	6	−14.3684 (−14.1610)
3e (Cl 2s)	4	−18.6638 (−18.4544)
$6a_1$ (Cl 2s)	2	−18.6638 (−18.4544)
$5a_1$ (O 1s)	2	−37.7021 (−37.8192)
2e (Mn $2p_x$, $2p_y$)	4	−46.4417 (−46.2746)
$4a_1$ (Mn $2p_z$)	2	−46.4417 (−46.2746)
$3a_1$ (Mn 2s)	2	−54.0284 (−53.8596)
1e (Cl 1s)	4	−201.5510 (−201.3576)
$2a_1$ (Cl 1s)	2	−201.5510 (−201.3576)
$1a_1$ (Mn 1s)	2	−468.3930 (−468.2048)
	Total 84	

[a] Levels below the dashed line are fully occupied in the ground state; those above the line are empty (12e is half-filled). Corresponding "free-atom" energy levels are shown in parentheses.

from the SCF–Xα calculation are listed in Table II. The core levels (Mn 1s, 2s, 2p; O 1s; Cl 1s, 2s, 2p) were included in the SCF–Xα calculation. However, only one symmetry orbital was used in the expansion of the molecular orbitals for these states. In Figure 2, we have plotted the eigenvalues for the "noncore" molecular orbitals along with the "noncore" levels of the free atoms (determined from SCF–Xα atomic calculations). The Xα ground-state eigenvalues for $MnOCl_3$ are plotted in Figure 3 together with the Xα eigenvalues for MnO_4^- [15] and MnO_3Cl in order to provide a comparison of related species. It is evident at this point that the ground-state eigenvalues for $MnOCl_3$ like those of MnO_3Cl have fallen into groups which allow one to identify each group by its parent tetrahedral partner. However, further comparison between the ground states of these two symmetry-related molecules is limited. The availability of p orbitals for the three chlorine atoms in $MnOCl_3$ gives rise to a set of normalized molecular orbitals (cf. Table I) different from the LCAO basis functions derived for the MnO_3Cl molecule.[13] One would expect, therefore, differences to occur in the charge density distribution for the ground state as well as differences in calculated transition-state energies.

The manganese in $MnOCl_3$ formally has a d^2 central metal configuration. The ground-state SCF–Xα calculation (cf. Figure 2) shows that the last two electrons making up this configuration are located in an orbital of e symmetry (12e). The $^3A_2(t_1^6e^2)$ ground state for $MnOCl_3$ correlates directly with that for the tetrahedral parent, MnO_4^{3-}.[10,11] However, the degeneracy of all orbitals of t (or states of T) symmetry will be reduced. Consequently, when one considers a one-

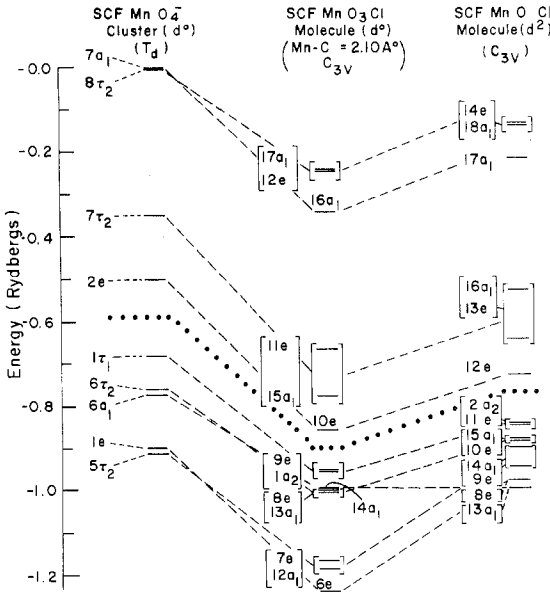

Figure 3. Comparison of the theoretical valence ground-state molecular eigenvalues of MnO_3Cl and $MnOCl_3$ in C_{3v} symmetry with the ground-state molecular eigenvalues of the SCF MnO_4^- cluster[15] in T_d symmetry. Orbitals below the dotted line are fully occupied while those above the line are unoccupied ($12e^2$ is half-occupied).

Table III. Transition State Energies for the Various Orbital Transitions in $MnOCl_3$ Grouped into a Tetrahedral Format Using the Non-Spin-Polarized Option in the SCF–Xα–SW Method

Orbital transitions		
T_d	C_{3v}	Energy, cm^{-1}
	Ligand Field	
$2e \rightarrow 3t_2$	$12e \rightarrow 13e$	9,450
	$12e \rightarrow 16a_1$	21,860
		Av 15,650
	Charge Transfer	
$t_1 \rightarrow 2e$	$2a_2 \rightarrow 12e$	16,300
	$11e \rightarrow 12e$	15,570
		Av 15,930
$6t_2 \rightarrow 2e$	$15a_1 \rightarrow 12e$	19,870
	$10e \rightarrow 12e$	20,160
		Av 20,020
$5t_2 \rightarrow 2e$	$14a_1 \rightarrow 12e$	21,940
	$9e \rightarrow 12e$	24,910
		Av 23,330
$1e \rightarrow 2e$	$8e \rightarrow 12e$	27,860
$6a_1 \rightarrow 2e$	$13a_1 \rightarrow 12e$	36,800
$1t_1 \rightarrow 7t_2$	$11e \rightarrow 13e$	24,120
	$2e_2 \rightarrow 13e$	24,670
		Av 24,400
	$11e \rightarrow 16a_1$	36,960
	$2a_2 \rightarrow 16a_1$	37,880
		Av 37,420
		Total av 30,910
$6t_2 \rightarrow 7t_2$	$10e \rightarrow 13e$	28,610
	$15a_1 \rightarrow 13e$	28,330
		Av 28,470
	$10e \rightarrow 16a_1$	41,580
	$15a_1 \rightarrow 16a_1$	41,420
		Av 41,500
		Total av 34,980
$5t_2 \rightarrow 7t_2$	$14a_1 \rightarrow 13e$	30,850
	$9e \rightarrow 13e$	33,820
		Av 32,330
	$14a_1 \rightarrow 16a_1$	44,300
	$9e \rightarrow 16a_1$	46,960
		Av 45,630
		Total av 38,980

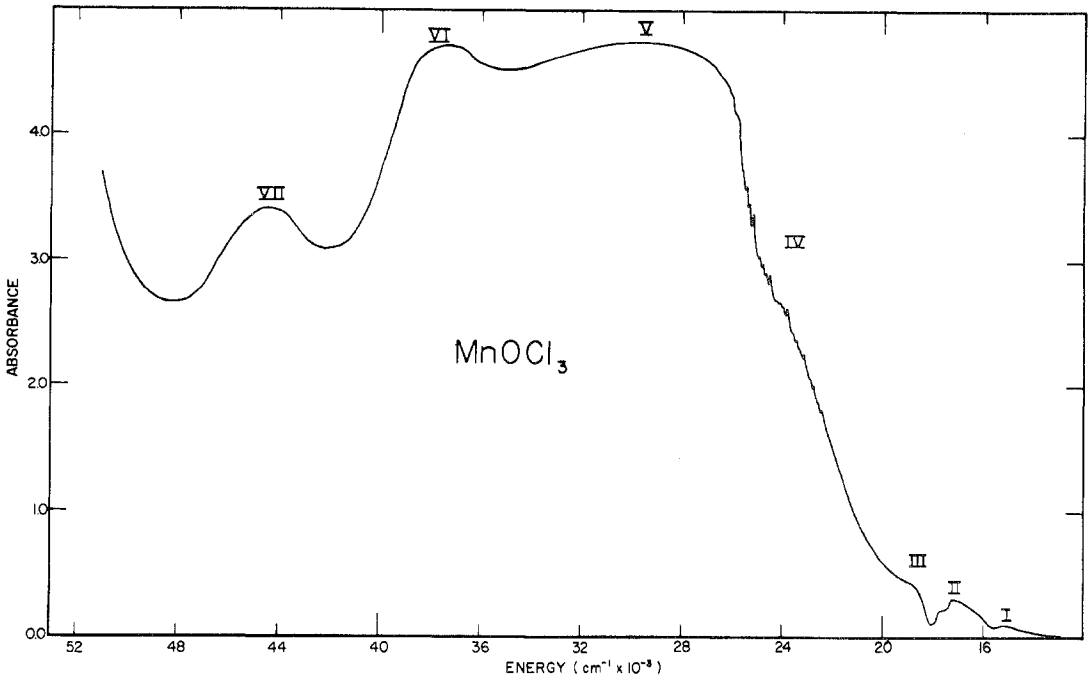

Figure 4. Gas-phase electronic absorption spectrum of $MnOCl_3$ in the region 12,000–52,000 cm^{-1}.

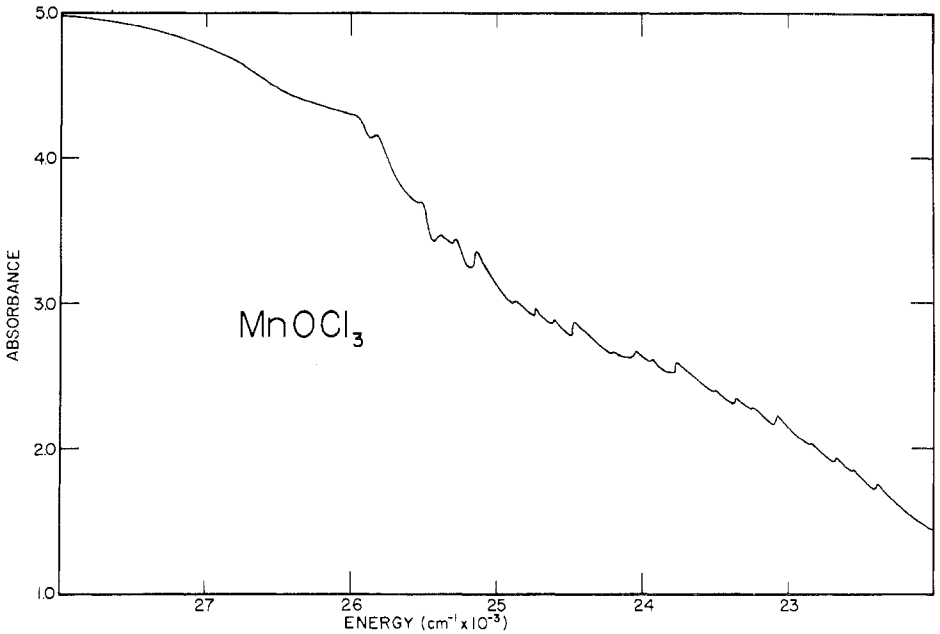

Figure 5. Vibrational structure in the 22,000–26,000-cm^{-1} region of the spectrum of $MnOCl_3$.

electron transfer from one of the "noncore" occupied (t) ground-state orbitals to the half-occupied (12e) or unoccupied (13e or $16a_1$) orbitals, the number of excited states possible is greater in C_{3v} symmetry than in the parent T_d symmetry. As a consequence of the selection rules for C_{3v} symmetry, any $^3A_2$, $^3E \leftarrow {}^3A_2$ transitions are electric dipole allowed while any $^3A_1 \leftarrow {}^3A_2$ transition is forbidden.

The Xα scattered-wave method does not give the total energy of a true many-electron state. Instead, it yields the energy center of gravity of the multiplet structure generated by the orbital excited configuration. The symmetry of $MnOCl_3$ is such that this center of gravity is not of an orbitally nondegenerate type. If we consider excitations that correspond to a $t_1 \rightarrow 2e$ transition in the parent tetrahedral molecule, we must then consider $e \rightarrow e$ and $a_2 \rightarrow e$ promotions in the C_{3v} case. While the $a_2 \rightarrow e$ excitation presents no problem, the $e \rightarrow e$ excitation produces the center of gravity of a triplet and singlet A_1, A_2, and E. The Xα–SW method in its present form cannot resolve this grouping of states for this symmetry.

However, as in our previous work,[13,14] we have determined the energy differences between the ground-state and various excited-state configurations by the non-spin-polarized transition-state calculation.[17] Thus, while we cannot separate out the excited states as completely as in our earlier work,[12] our calculation for these excitations (cf. Table III) is of considerable value in the interpretation of the electronic absorption spectrum of $MnOCl_3$.

Experimental Section

Manganese oxide trichloride was prepared by the method of Briggs.[22] Purification was achieved using techniques previously reported.[13,14] The optical spectrum was obtained with a resolution of ~10 cm^{-1}. Maintenance of the gas at 0 → 5° during the optical measurement was necessary in order to prevent decomposition of the $MnOCl_3$.

Table IV. Assignments for $MnOCl_3$

Band	Energy, cm^{-1} Obsd	Energy, cm^{-1} Calcd	State transition C_{3v}	Orbital transition T_d	Orbital transition C_{3v}
I	15,000	9,450	$\left[{}^1A_2, {}^3A_2 \overset{z}{\leftarrow} {}^3A_2\right]$ $\left[{}^1E, {}^3E \overset{xy}{\leftarrow} {}^3A_2\right]$	$2e \rightarrow 7t_2$	$12e \rightarrow 13e$
II	17,500	16,300	${}^1E, {}^3E \overset{xy}{\leftarrow} {}^3A_2$	$t_1 \rightarrow 2e$	$2a_2 \rightarrow 12e$
	(17,000)	15,570	$\left[{}^1A_2, {}^3A_2 \overset{z}{\leftarrow} {}^3A_2\right]$ $\left[{}^1E, {}^3E \overset{xy}{\leftarrow} {}^3A_2\right]$		$11e \rightarrow 12e$
III	19,000	19,870	${}^1E, {}^3E \overset{xy}{\leftarrow} {}^3A_2$	$6t_2 \rightarrow 2e$	$15a_1 \rightarrow 12e$
		20,160	$\left[{}^1A_2, {}^3A_2 \overset{z}{\leftarrow} {}^3A_2\right]$ $\left[{}^1E, {}^3E \overset{xy}{\leftarrow} {}^3A_2\right]$		$10e \rightarrow 12e$
		21,860	${}^1E, {}^3E \overset{xy}{\leftarrow} {}^3A_2$	$2e \rightarrow 7t_2$	$12e \rightarrow 16a_1$
		21,940	${}^1E, {}^3E \overset{xy}{\leftarrow} {}^3A_2$	$5t_2 \rightarrow 2e$	$14a_1 \rightarrow 12e$
IV	24,000	24,910	$\left[{}^1A_2, {}^3A_2 \overset{z}{\leftarrow} {}^3A_2\right]$ $\left[{}^1E, {}^3E \overset{xy}{\leftarrow} {}^3A_2\right]$	$5t_2 \rightarrow 2e$	$9e \rightarrow 12e$
		24,670	${}^1E, {}^3E \overset{xy}{\leftarrow} {}^3A_2$	$1t_1 \rightarrow 7t_2$	$2a_2 \rightarrow 13e$
		24,120	$\left[{}^1A_2, {}^3A_2 \overset{z}{\leftarrow} {}^3A_2\right]$ $\left[{}^1E, {}^3E \overset{xy}{\leftarrow} {}^3A_2\right]$		$11e \rightarrow 13e$
V	28,000–37,000	27,860	$\left[{}^1A_2, {}^3A_2 \overset{z}{\leftarrow} {}^3A_2\right]$ $\left[{}^1E, {}^3E \overset{xy}{\leftarrow} {}^3A_2\right]$	$1e \rightarrow 2e$	$8e \rightarrow 12e$
		28,330	${}^1E, {}^3E \overset{xy}{\leftarrow} {}^3A_2$	$6t_2 \rightarrow 7t_2$	$15a_1 \rightarrow 13e$
		28,610	$\left[{}^1A_2, {}^3A_2 \overset{z}{\leftarrow} {}^3A_2\right]$ $\left[{}^1E, {}^3E \overset{xy}{\leftarrow} {}^3A_2\right]$		$10e \rightarrow 13e$
		30,850	${}^1E, {}^3E \overset{xy}{\leftarrow} {}^3A_2$	$5t_2 \rightarrow 7t_2$	$14a_1 \rightarrow 13e$
		33,820	$\left[{}^1A_2, {}^3A_2 \overset{z}{\leftarrow} {}^3A_2\right]$ $\left[{}^1E, {}^3E \overset{xy}{\leftarrow} {}^3A_2\right]$		$9e \rightarrow 13e$
VI	38,000	36,800	${}^1E, {}^3E \overset{xy}{\leftarrow} {}^3A_2$	$6a_1 \rightarrow 2e$	$13a_1 \rightarrow 12e$
		36,960	${}^1E, {}^3E \overset{xy}{\leftarrow} {}^3A_2$	$1t_1 \rightarrow 7t_2$	$11e \rightarrow 16a_1$
		37,880	${}^1A_2, {}^3A_2 \overset{z}{\leftarrow} {}^3A_3$		$2a_2 \rightarrow 16a_1$
		41,580	${}^1E, {}^3E \overset{xy}{\leftarrow} {}^3A_2$	$6t_2 \rightarrow 7t_2$	$10e \rightarrow 16a_1$
VII	45,000	46,960	${}^1E, {}^3E \overset{xy}{\leftarrow} {}^3A_2$	$5t_2 \rightarrow 7t_2$	$9e \rightarrow 16a_1$

Results

The electronic absorption spectrum of $MnOCl_3$ at approximately 5° is shown in Figures 4 and 5. This spectrum is seen to consist of seven separate areas of absorption: (1) a weak structureless band (I) centered at ~15,200 cm^{-1}, (2) a more intense band (II), centered at ~17,200 cm^{-1}, with a less intense shoulder on the high-energy side at ~18,000 cm^{-1}, (3) a slightly more intense, broad band (III) centered at ~19,000 cm^{-1}, (4) an intense, broad, structured shoulder centered at ~24,000 cm^{-1} (band IV), (5) an extremely intense, broad band (V) between ~26,000 and ~35,000 cm^{-1}, (6) an intense broad band (VI) centered at ~38,000 cm^{-1}, and (7) a broad band (VII) with approximately three-fourths of the intensity of bands V and VI centered at ~44,000 cm^{-1}. The intensity ratio of bands I–VII in order of increasing energy is approximately 0.10:0.25:0.35:2.75:4.75:4.75:3.50.

Absolute ϵ values for the optical density of the recorded spectrum could not be obtained from this experiment.

The line shape of band V does not resemble that of a gaussian curve. However, its reproducibility via several measurements leads us to believe in its authenticity. Therefore, one can only suggest from the electronic assignments discussed later that this apparent distortion may be caused by the extensive overlap of excited states in this region.

Discussion

Electronic Assignment. A comparison of the $X\alpha$ ground-state molecular orbitals of the d^0 MnO_4^- cluster vs. the d^0 MnO_3Cl and d^1 MnO_2Cl_2 molecules[13,14] and with those of the d^2 $MnOCl_3$ molecule (cf. Figure 3) strongly suggests that many of the optical properties of the MnO_4^{x-} (x = 1–3) ions can be understood in terms of their halide-substituted, symmetry-reduced daughter species. It also agrees with the

suggestion of Orgel[23] that the electronic structure of the various MnO_4^{x-} ions can be understood in terms of the structure of the MnO_4^- ion.[24,25]

The assignments of bands I–VII based upon our SCF–Xα–SW calculation are given in Table IV. Band I is assigned to the 12e → 13e component of the parent 2e → 7t2 ligand field excitation giving rise to two electric dipole allowed transitions, $^3A_2$, $^3E \leftarrow {}^3A_2$, and two spin-forbidden transitions, $^1A_2$, $^1E \leftarrow {}^3A_2$. The other ligand field component, 12e → 16a1, giving rise to the ^1E, $^3E \leftarrow {}^3A_2$ transitions appears to be buried within the manifold of band III. The spin-forbidden singlet states are included in the assignments in Table IV as the singlet–triplet splitting could not be determined in our calculation and insufficient structure is present in this manifold to allow us experimentally to identify the various spin-allowed and spin-forbidden components. The singlet–triplet splitting for the d^0 MnO_3Cl molecule was ~2200 cm^{-1} in this region.[13] Assuming the same order of magnitude triplet–singlet splitting in $MnOCl_3$, the singlets appear to be buried beneath the dominant triplets in each of the seven bands in the optical spectrum.

Band II located at ~17,000 cm^{-1} with a shoulder at ~17,500 cm^{-1} is assigned to the $^3A_2$, $^3E \leftarrow {}^3A_2$ and $^3E \leftarrow {}^3A_2$ transitions from the 11e → 12e and 2a2 → 12e excitations, respectively. These correlate with the t1 → 2e charge-transfer transition of the T_d parent. However, since the intensity of band II is only slightly greater than that of band I (0.25 vs. 0.10), the possibility of some d–d mixing in this region, as well as in band III, appears quite likely. This observation in bands I–III coincides with the assignments of Milstein et al.[10,11] for the optical spectrum of MnO_4^{3-}.

In band III our SCF–Xα calculation indicates an overlapping set of excited-state transitions arising from the 14a1, 15a1, 10e → 12e excitations. These correlate with the 6t2, 5t2 → 2e allowed charge-transfer excitations in the parent T_d molecule. Also included is the 12e → 16a1 component which correlates with the ligand field 2e → 7t2 excitation discussed earlier.

Based upon intensity considerations of the optical spectrum and our SCF–Xα transition-state energies (cf. Table IV), the shoulder at ~24,000 cm^{-1}, band IV, the broad intense band (V) between ~28,000 and ~37,000 cm^{-1}, and the two intense bands centered at ~38,000 and ~45,000 cm^{-1} are primarily charge transfer in origin. Whether or not all of the states indicated in Table IV are present in these regions is difficult to ascertain from our study. However, comparison of the intensities of band VII vs. bands V and VI with the calculated number of spin and electric dipole allowed transitions in these regions (1 vs. 8 and 4: Table IV) correlates quite well with the amount of charge transfer assigned to these bands.

Vibrational Assignment. Assignments of the observed excited-state frequencies for $MnOCl_3$ have been made using reported ground-state frequencies for $VOCl_3$[19,20] [ν1(a1) = 1035 cm^{-1}; ν2(a1) = 408 cm^{-1}; ν3(a1) = 165; ν4(e) = 504 cm^{-1}; ν5(e) = 249 cm^{-1}; ν6(e) = 129 cm^{-1}] because the fundamental frequencies for manganese oxide trichloride have not yet been reported. Since $MnOCl_3$ is isostructural with $VOCl_3$ and since vanadium is only slightly more electronegative than manganese (1.6 vs. 1.5), one would expect the fundamental frequencies of $MnOCl_3$ to be near the values for $VOCl_3$.

The well-defined vibrational structure in the region from ~22,300 to ~26,000 cm^{-1} (cf. Figure 5) consists of two electronic origins separated by 280 cm^{-1} (cf. Table V). The first system with its origin at 22,396 cm^{-1} contains five parent members uniformly spaced at ~683 cm^{-1}. Built upon each parent line is a weaker satellite line at an average of ~154 cm^{-1} higher in energy. The second system with its origin at 22,676 cm^{-1} consists of five parent members spaced at ~680 cm^{-1} with a weaker satellite member built upon each parent at ~153 cm^{-1} to higher energy.

Table V. Vibrational Components in the 22,000–26,000-cm^{-1} Region of the Spectrum of $MnOCl_3$

$\bar{\nu}$, cm^{-1}	Assignment	$\Delta\bar{\nu}$, cm^{-1}
22,396	$1\nu_0$	
22,558	$1\nu_0 + \nu_3$	152
22,676	$2\nu_0$	
22,847	$2\nu_0 + \nu_3$	171
23,084	$1\nu_0 + \nu_1$	689
23,250	$1\nu_0 + \nu_1 + \nu_3$	164
23,359	$2\nu_0 + \nu_1$	683
23,513	$2\nu_0 + \nu_1 + \nu_3$	154
23,770	$1\nu_0 + 2\nu_1$	685
23,929	$1\nu_0 + 2\nu_1 + \nu_3$	159
24,044	$2\nu_0 + 2\nu_1$	685
24,212	$2\nu_0 + 2\nu_1 + \nu_3$	169
24,456	$1\nu_0 + 3\nu_1$	686
24,606	$1\nu_0 + 3\nu_1 + \nu_3$	150
24,728	$2\nu_0 + 3\nu_1$	684
24,876	$2\nu_0 + 3\nu_1 + \nu_3$	148
25,135	$1\nu_0 + 4\nu_1$	679
25,288	$1\nu_0 + 4\nu_1 + \nu_3$	153
25,394	$2\nu_0 + 4\nu_1$	666
25,519	$2\nu_0 + 4\nu_1 + \nu_3$	125
25,813	$1\nu_0 + 5\nu_1$	678
25,965	$1\nu_0 + 5\nu_1 + \nu_3$	152

	Av, cm^{-1}		
	System I	System II	Total av, cm^{-1}
ν_1	683	680	682
ν_3	155	153	154

Table VI. Distribution of Electronic Charge in the $MnOCl_3$ Molecule[a]

Symmetry	Mn sphere	O sphere	Cl sphere	Interatomic region	Extramolecular region
14e	0.0009	0.0140	0.0507	0.6544	0.2801 p, d
18a1	0.0012	0.0059	0.0624	0.6465	0.2842 p
17a1	0.0011	0.0075	0.0534	0.7150	0.2230 s
16a1	0.5238 d	0.2452 p	0.0759	0.1524	0.0027
13e	0.5012 d	0.0799 p	0.3117 p	0.1136	0.0059
12e	0.5957 d	0.1165 p	0.1692 p	0.1170	0.0017
2a2	0.0003	0.0000	0.9024 p	0.0932	0.0041
11e	0.0054	0.1311 p	0.7417 p	0.1284	0.0034
15a1	0.0044	0.0345 p	0.8130 p	0.1444	0.0038
10e	0.0078	0.0922 p	0.7380 p	0.1567	0.0055
14a1	0.0294	0.0442 p	0.8049 p	0.1106	0.0109
9e	0.3282 d	0.0873 p	0.4527 p	0.1286	0.0032
8e	0.3770 d	0.1964 p	0.2751 p	0.1489	0.0027
13a1	0.3815 d	0.3951 p	0.0486 p	0.1742	0.0007

Total Electronic Charge[b]

Mn sphere	−22.7885	Interatomic region	−4.4001
O sphere	−6.6585	Extramolecular region	−0.1124
Cl sphere	−50.0406	Total charge	−84.0001

[a] Contribution of each normalized valence orbital in the ground state to a unit of electronic charge in the various regions of the molecule $MnOCl_3$. The underlined accompanying symbol (s, p, d, or f) indicates the orbital type in which the majority of the charge density resides. The charges associated with each molecular orbital are weighted by the occupancy of that orbital. The contribution from the ligands are weighted by the number of atoms of each type. Orbitals below the dashed line are fully occupied. Those above the line are unoccupied (12e is half-occupied). [b] Obtained from the summing of charge densities in all occupied molecular orbitals (including core orbitals) in the ground state.

The average frequencies 682 and 154 cm^{-1} (cf. Table V) observed in band IV are assigned to the ν_1 and ν_3 modes, respectively. These represent reductions of ~34% (ν_1) and ~7% (ν_3) in the excited states.

The charge density distribution (Table VI) for the excitations assigned to this region (band IV) show the majority of charge

to be located on the chlorine atoms in the ground-state $2a_2$, $11e$ (t_1) and $14a_1$, $9e$ ($6t_2$) molecular orbitals. Therefore, the appearance of the ν_3 satellite mode is expected. However, the presence of the ν_1 mode indicates a strong oxide character in either the $9e \rightarrow 12e$ component of the $5t_2 \rightarrow 2e$ excitation (T_d parentage) or the $2a_2$, $11e \rightarrow 13e$ components of the $1t_1 \rightarrow 7t_2$ excitation (T_d parentage). This is unexpected considering the charge density distribution in the orbitals comprising these excitations (cf. Table VI). However, such behavior is observed for the $5t_2 \rightarrow 2e$ excitations in MnO_3Cl and MnO_2Cl_2. The $L \rightarrow M$ charge transfer assigned to this region is therefore a $p\pi \rightarrow d\pi^*$ (chlorine → manganese) interaction with some $p\pi \rightarrow d\pi^*$ (chlorine → oxygen or chlorine → manganese) charge transfer also likely.

Acknowledgment. The authors wish to acknowledge the support of the National Science Foundation (Grants GP-15432A1 and GP-41506) and the Research Corp. Dr. John H. Wood is thanked for providing the SCF–Xα–SW computer program used in our molecular orbital calculations.

Registry No. $MnOCl_3$, 23097-77-0.

References and Notes

(1) A. Carrington and M. C. R. Symons, *J. Chem. Soc.*, 3373 (1956).
(2) A. Carrington, D. J. Ingram, K. A. K. Lott, D. S. Schonland, and M. C. R. Symons, *J. Chem. Soc.*, 101 (1959).
(3) A. Carrington and D. S. Schonland, *Mol. Phys.*, **3**, 331 (1960).
(4) P. D. Johnson, J. S. Prener, and J. D. Kingsley, *Science*, **141**, 1179 (1963).
(5) R. F. Fenske and C. C. Sweeney, *Inorg. Chem.*, **3**, 1105 (1964).
(6) J. D. Kingsley, J. S. Prener, and B. Segall, *Phys. Rev.* [*Sect.*] *A*, **137**, 189 (1965).
(7) M. Greenblatt, E. Banks, and B. Post, *Acta Crystallogr.*, **23**, 166 (1967).
(8) B. Krebs, A. Müller and H. W. Roesky, *Mol. Phys.*, **12**, 469 (1967).
(9) D. K. Nath and F. A. Hummel, *J. Am. Ceram. Soc.*, **52**, 8 (1969).
(10) J. Milstein and S. L. Holt, *Inorg. Chem.*, **8**, 1021 (1969).
(11) J. B. Milstein, J. Ackerman, S. L. Holt, and B. R. McGarvey, *Inorg. Chem.*, **11**, 1178 (1972).
(12) J. P. Jasinski, J. H. Wood, S. L. Holt, and L. B. Asprey, in press.
(13) J. P. Jasinski, J. H. Wood, S. L. Holt, and J. Moskowitz, in press.
(14) J. P. Jasinski and S. L. Holt, in press.
(15) K. H. Johnson and F. C. Smith, Jr., *Chem. Phys. Lett.*, **10**, 219 (1971).
(16) K. H. Johnson, *J. Chem. Phys.*, **45**, 3085 (1966); K. H. Johnson and F. C. Smith, Jr., *Phys. Rev. B*, **5**, 831 (1972); K. H. Johnson and F. C. Smith, Jr., *Chem. Phys. Lett.*, **7**, 541 (1970).
(17) J. C. Slater and K. H. Johnson, *Phys. Rev. B*, **5**, 844 (1972).
(18) J. C. Slater, "Quantum Theory of Molecules and Solids", Vol. 4, McGraw-Hill, New York, N.Y., 1974.
(19) J. J. Eichoff and F. Weigel, *Z. Anorg. Allg. Chem.*, **275**, 267 (1954).
(20) F. A. Miller and L. R. Cousins, *J. Chem. Phys.*, **26**, 329 (1957).
(21) K. H. Schwarz, *Phys. Rev. B*, **5**, 2466 (1972).
(22) T. S. Briggs, *J. Inorg. Nucl. Chem.*, **30**, 2866 (1968).
(23) L. E. Orgel, *Mol. Phys.*, **7**, 397 (1964).
(24) M. Wolfsberg and L. Helmholz, *J. Chem. Phys.*, **20**, 837 (1952).
(25) C. J. Ballhausen and A. D. Liehr, *J. Mol. Spectrosc.*, **2**, 342 (1958).

Contribution from Chemical Abstracts Service,
The Ohio State University, Columbus, Ohio 43210

Stereochemical Notation in Coordination Chemistry. Mononuclear Complexes

MARY F. BROWN,[1] BILLY R. COOK, and THOMAS E. SLOAN*

Received September 9, 1974 AIC40635L

A unified system of notation for geometric isomers, including central atom symmetry and optical isomers for mononuclear complexes, is presented for known geometries up to coordination number 6. This notation system makes extensive use of the complementary features of the Cahn, Ingold, and Prelog (CIP) system for tetrahedra, the IUPAC helical system for bis- and tris-chelated octahedra, and a proposal by Petrarca, Rush, and Brown using CIP priority ranking to describe stereoelements in a unified and general manner. This system has been introduced in the Indexes to *Chemical Abstracts* starting with Volume 76 (January–June 1972). Certain aspects of ligand stereochemistry and the notation for ferrocene complexes are discussed.

Introduction

The concept of the geometric arrangement of groups around a central atom or ion has been a central precept of coordination theory since its early development by Alfred Werner starting in 1893. The ideas of coordination number and the specific geometric arrangement of ligands (symmetry) are among the first encountered by the student of coordination chemistry. In a verbal discussion between coordination chemists, the terms "square planar", "octahedral", and "tetrahedral" are as often heard as "isomer", "molecule", or "ion". Formal nomenclature, however, has skirted the development of names or notations which give explicit designations to the symmetry of a complex. Thus, when the coordination chemist writes *cis*-diamminedichloroplatinum, previous chemical experience and logic imply that the compound has a square-planar configuration. The indirect implication of the configuration of a complex has not greatly hindered formal communication in coordination chemistry up to now because one type of symmetry predominated, except for coordination numbers 4 and 5. In these latter two instances experience in the area led to generalizations of the accepted symmetries in a specific system and the exceptions to the generalizations became well known. However, with the growth of coordination chemistry in the last three decades, the number of symmetries and notations proposed and used in formal communication has increased to match the growth in the field.

In the recent literature, various stereochemical notations for coordination compounds have been suggested.[2-11] The most general systematic approach to stereochemical notation is the Cahn–Ingold–Prelog (CIP) standard sequence rule[7] which has been used with great success for the several classes of chirality encountered in organic chemistry.

The standard sequence rule is the procedure in which the ligands are ranked in order of precedence, hereafter referred to as seniority, on the three-dimensional model of the molecule. The chiral element is given a symbol representing the handedness of the progression of the seniorities of the ligands. For the case of the nearly tetrahedral carbon center encountered frequently in organic chemistry, the molecule is viewed from the side opposite the least-senior (largest priority number) ligand and the symbols *R* (right-handed or clockwise) and *S* (left-handed or anticlockwise) are used to indicate the direction of the progression of the seniorities.

The seniorities are determined according to the subrules given in ref 7: (1) higher atomic number precedes lower; (2) higher atomic mass number precedes lower; (3) *Z* precedes *E*;[12] (4) like pair *R*,*R* or *S*,*S* precedes unlike *R*,*S* or *S*,*R*; ...; (5) *R* precedes *S*....

In the application of these subrules the ligands are arranged in order of decreasing atomic number. For the case of a tetracoordinate center with the ligands H, Cl, Br, and F, the ligands are ranked 35 > 17 > 9 > 1, Br > Cl > F > H, and the relative priority numbers Br = 1, Cl = 2, F = 3, and H = 4 are used to determine the clockwise or anticlockwise sense